Dalton Transactions

Chromophore-labelled, luminescent platinum complexes: syntheses, structures, and spectroscopic properties

Journal:	*Dalton Transactions*
Manuscript ID	DT-ART-04-2016-001335.R4
Article Type:	Paper
Date Submitted by the Author:	23-May-2016
Complete List of Authors:	Pope, Simon; University of Cardiff, School of Chemistry Stacey, Oliver; Cardiff University, Ward, Benjamin; Cardiff University, School of Chemistry Horton, Peter; Southampton UNiversity, Chemistry Coles, Simon; Southampton, Chemistry

Cite this: DOI: 10.1039/c0xx00000x

www.rsc.org/xxxxxx

ARTICLE TYPE

Chromophore-labelled, luminescent platinum complexes: syntheses, structures, and spectroscopic properties

Oliver J. Stacey,[a] Benjamin D. Ward,[a] Simon J. Coles,[b] Peter N. Horton[b] and Simon J. A. Pope[a]*

Received (in XXX, XXX) Xth XXXXXXXXX 20XX, Accepted Xth XXXXXXXXX 20XX

DOI: 10.1039/b000000x

Ligands based upon 4-carboxamide-2-phenylquinoline derivatives have been synthesised with solubilising octyl hydrocarbon chains and tethered aromatic chromophores to give naphthyl (**HL^2**), anthracenyl (**HL^3**) and pyrenyl (**HL^4**) ligand variants, together with a non-chromophoric analogue (**HL^1**) for comparison. ^{1}H NMR spectroscopic studies of the ligands showed that two non-interchangeable isomers exist for **HL^2** and **HL^4** while only one exists for **HL^1** and **HL^3**. Supporting DFT calculations on **HL^4** suggest that the two isomers may be closely isoenergetic with a relatively high barrier to exchange of *ca.* 100 kJmol^{-1}. These new ligands were cyclometalated with Pt(II) to give complexes [Pt(**L$^{1\text{-}4}$**)(acac)] (acac = acetylacetonate). The spectroscopically characterised complexes were studied using multinuclear NMR spectroscopy including ^{195}Pt{^{1}H} NMR studies which revealed δ_{Pt} *ca.* -2785 ppm for [Pt(**L$^{1\text{-}4}$**)(acac)]. X-ray crystallographic studies were undertaken on [Pt(**L^3**)(acac)] and [Pt(**L^4**)(acac)], each showing the weakly distorted square planar geometry at Pt(II); the structure of [Pt(**L^3**)(acac)] showed evidence for intermolecular Pt-Pt interactions. The UV-vis. absorption studies show that the spectral profiles for [Pt(**L$^{2\text{-}4}$**)(acac)] are a composite of the organic chromophore centred bands and a broad ^{1}MLCT ($5d\rightarrow\pi^*$) band (*ca.* 440 nm) associated with the complex. Luminescence studies showed that complexes [Pt(**L$^{2\text{-}4}$**)(acac)] are dual emissive with fluorescence characteristic of the tethered fluorophore and long-lived phosphorescence attributed to ^{3}MLCT emission. In the case of the pyrenyl derivative, [Pt(**L^4**)(acac)], the close energetic matching of the ^{3}MLCT and ^{3}LC$_{pyr}$ excited states led to an elongation of the ^{3}MLCT emission lifetime (τ = 42 μs) under degassed solvent conditions, suggestive of energy transfer processes between the two states.

Introduction

Chromophore-appended, luminescent transition metal complexes have enjoyed significant attention over the years due to the wide variety of both fundamental and applied studies that are possible with such systems.[1] The interactions of photoactive units, be they covalently linked in simple dyad systems or self-assembled into supramolecular architectures, can allow studies into electron[2] and energy transfer[3] mechanisms, triplet-triplet annihilation and upconversion.[4] The interplay between chromophore-localized and complex-based excited states has been commonly studied with a range of d^6 and d^8 heavy metal transition metals including, most commonly, Ru(II).

The use of pyrene as a photoactive unit in such systems has also attracted particular attention. Highly structured monomer-type fluorescence at 320-400 nm, an unstructured broad excimer-type emission at 430-460 nm and long-lived phosphorescence at around 600 nm dominate the emission properties of pyrene and have led to wide applications, particularly in sensing.[5] A large number of studies have investigated the photophysical properties of luminescent complexes that incorporate pyrene chromophore(s) into the ligand architecture; a recent article has reviewed metal-pyrene assemblies and their photophysical properties.[6]

Some reports have also focused on pyrene-derived ligands as cyclometalating components within Ir(III)[7] and Pt(II) complexes,[8] leading to the heavy metal mediated population of ligand-centred triplet states. Such species have been shown to possess a range of luminescent properties and can also display highly efficient singlet oxygen (^{1}O$_2$) photogeneration.[9]

Of relevance to this paper are the reports of complexes that incorporate tethered chromophores *via* a linking (or spacer) bridge, and complexes that show extended luminescent lifetimes due to the *energy reservoir* effect (sometimes also referred to as *reversible electronic energy transfer*), arising through thermal equilibration between triplet metal-to-ligand charge transfer (^{3}MLCT) and triplet ligand-centred pyrene (^{3}LC$_{pyr}$) excited states.[10] The requirement for this reversible triplet-triplet energy transfer is that the two excited states must lie in close energetic proximity, the observable manifestation of which leads to elongated ^{3}MLCT lifetimes. Pyrene-appended diimine complexes of Ru(II) are the classical examples in this context: the ^{3}MLCT lifetime of the [Ru(bpy)$_3$]$^{2+}$ chromophore can be extended well into the microsecond domain by excited state equilibration with long-lived ^{3}LC$_{pyr}$ where the energetic difference in the states is *ca.* 600 cm^{-1}.[11] Although Ru(II) diimine systems represent the

vast majority of the reported examples that show elongated ^{3}MLCT lifetimes *via* this mechanism, studies have also looked at pyrene-appended cyclometalated Ir(III) species which also show remarkable extension of lifetimes and high sensitivity to dissolved $^3O_2$.[12] The energy difference of the two interacting states was 680 cm^{-1} and led to a very long lifetime of 225 μs for the complex. Subsequent studies have further developed Ir(III) complexes to yield high sensitivity optical oxygen sensors through their incorporation into nanostructured metal-oxide matrix films.[13]

The majority of Pt(II) complexes that incorporate a pyrene moiety into the ligand fragment show $^3LC_{pyr}$ based phosphorescence because this triplet state often lies below any ^{3}MLCT state associated with the Pt(II)-based chromophore. Acetylide complexes of Pt(II) which possess conjugated pyrene units are a typical example where the long-lived, room temperature emission can be solely attributed to $^3LC_{pyr}$.[14] The group of McMillin has reported cyclometalated Pt(II) complexes that incorporate a 4-substituted 2,2′:6′,2″-terpyridine (trpy) ligand wherein the conjugated, pyrene-appended complex shows a long lifetime of 45 μs in fluid solution. However, this lifetime was not attributed to energy reservoir effects, but rather the predominance of $^3LC_{pyr}$ character to the emitting state.[15] In earlier work the same group reported a similar trpy-pyrene Pt(II) compound and attributed the long luminescent lifetime of the complex to an excited state of mixed ^{3}ILCT/$^3LC_{pyr}$/^{3}MLCT parentage, although the possibility of excited state equilibrium between the ^{3}ILCT and $^3LC_{pyr}$ states, by anology with earlier discussion, could not be ruled out.[16] Zhao and Guo have reported Schiff base complexes of Pt(II) that include conjugated pyrene chromophores and one of these complexes possesses luminescent properties that appear to be consistent with a ^{3}MLCT/$^3LC_{pyr}$ thermal equilibration giving extended lifetimes in the microsecond domain.[17]

To the best of our knowledge all of the pyrene-platinum dyads reported thus far all involve direct conjugation of the pyrene unit to the chelating ligand and/or direct coordination to the platinum centre. We therefore report the first series of functionalised cyclometalated Pt(II) complexes, [Pt(**L^n**)(acac)] based upon a substituted 4-carboxamido-2-phenylquinoline ligand, that incorporate a tethered chromophore (naphthyl, anthracenyl and pyrenyl) and builds on our prior work on cyclometalated luminescent Pt(II) species that encompass the 4-substituted, 2-phenylquinoline moiety.[18] Crucially in such complexes the emitting state of the Pt(II) complexes is primarily ^{3}MLCT in character with a tuneable emission wavelength around 610-630 nm (*cf* [Ru(bpy)$_3$](PF$_6$)$_2$ emits at 615 nm[19] in MeCN). Therefore such species should be viable candidates for probing energy reservoir effects with selected chromophores such as pyrene. In this study, the complexes are further adorned with a lipophilic octyl hydrocarbon chain to enhance the solubility properties of the ligand precursors and enable study of the Pt(II) coordination chemistry. This paper discusses the synthetic routes, characterisation, including X-ray crystal structures, and luminescence properties of these new ligands and complexes.

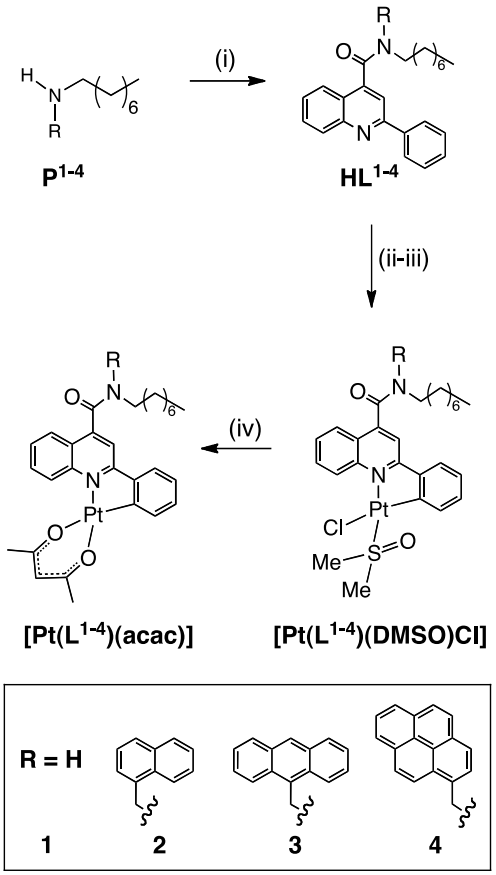

Scheme 1. Synthetic route to the ligands and platinum complexes. (i) 2-phenylquinoline-4-carbonyl chloride, $CHCl_3$; (ii) K_2PtCl_4, H_2O, $EtO(CH_2)_2OH$; (iii) DMSO; (iv) sodium acetylacetonate, 3-pentanone.

Results and Discussion

Synthesis and characterisation of the ligands

Initially syntheses of chromophoric ligands lacking the alkyl chain were attempted *via* condensation of different chromophoric amino precursors (*e.g.* 1-aminonaphthalene, 1-aminomethylpyrene) with 2-phenylquinoline-4-carbonyl chloride. However, the resultant ligands were found to be insoluble in all common solvents other than DMSO and subsequent attempts to synthesise the corresponding Pt(II) dimers were unsuccessful using established methodologies. To overcome the limiting solubility of these species an alternative target was sought that incorporated an alkyl chain into the ligand architecture (Scheme 1). Thus, the precursor secondary amines (**P$^{2\text{-}4}$**) were formed from the reductive amination of 1-octylamine (**P^1**) with the aryl aldehyde of the corresponding chromophore (1-naphthaldehyde, 9-anthracenecarboxaldehyde, 1-pyrenecarboxaldehyde). **P$^{2\text{-}4}$** were then reacted with 2-phenylquinoline-4-carbonyl chloride to form the corresponding ligands **HL$^{2\text{-}4}$** in good yields. The chromophore-free analogue **HL^1** was synthesised by condensing 1-octylamine with 2-phenylquinoline-4-carbonyl chloride and has been reported previously.[17b]

Characterisation of these new ligands was achieved using a

variety of standard techniques. In the ^{1}H NMR spectra of the ligands a number of identifying features were observed. Upon comparison with the data for **HL^1**, for **HL^3** the methylene group linking the anthracenyl unit to the amide group appeared as a set of diastereotopic signals centred *ca.* 6.05 ppm (with a geminal coupling constant of $^2J_{HH}$ = 15.2 Hz), suggesting a rigid conformation of a single isomer with limited rotation of the anthracenyl moiety. In the corresponding spectra of **HL^2** and **HL^4**, the same methylene group revealed two distinct sets (SI, Fig. S1) of diastereotopic protons (in an approximate 2:1 ratio), suggesting that there were two distinct isomeric forms of these ligands, attributed to restricted rotation about the amide bond. The major isomer displayed two distinct doublets with a geminal coupling constant $^2J_{HH}$ ~ 15 Hz, the minor isomer a much broader, less resolved signal. The presence of two isomers in **HL^2** and **HL^4** leads to a highly complex set of overlapping aromatic signals. In our hands these isomers were found to be inseparable using column chromatography.

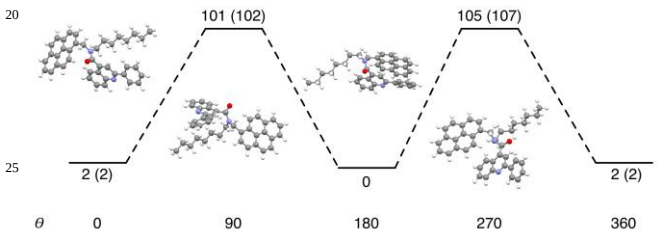

Figure 1. Calculated relative enthalpies (free energies in kJmol^{-1}) of ligand **HL^4** as a function of the dihedral angle θ (O–C–N–C$_{pyrene}$).

Conformational analysis of the isomeric forms of HL^4

Since the ligand contains an amide linkage, there is a possibility of significant delocalization of the $\pi_{(C=O)}$ and N_π orbitals; disruption of this delocalization is therefore expected to give rise to restricted rotation about the amide bond. The presence of an unsymmetrical quinoline amide substituent means that the two in-plane amide orientations correspond to two different isomeric forms. We probed the energetics by which these two isomers could interconvert using computational methods. A relaxed potential energy surface scan, obtained by systematically varying the amide O–C–N–C$_{pyrene}$ dihedral angle, whilst allowing the remaining centers to optimize, afforded an energy profile similar to that displayed in Fig. 1. As expected, the energy profile shows two minima, corresponding to approximate dihedral angles of 0 ° and 180 °, *i.e.* structures in which the N_π lone pair can be considered delocalized over the amide group. In addition, the energy profile contains two maxima, corresponding to the two perpendicular arrangements of the amide group, in which the $\pi_{(C=O)}$ and N_π orbitals are orthogonal.

Taking structures along the calculated potential energy surface as suitable starting points, the minima and transition state structures were optimized without geometry restraints, and their relative energies obtained (Fig. 1). As expected, the two minima correspond to structures in which the O–C–N–C$_{pyrene}$ dihedral angles are approximately 0 ° and 180 ° (optimized values are –1 ° and 175 ° respectively), consistent with qualitative predictions. Likewise, the two transition states were found to have dihedral angles of 103 ° and 293 °, somewhat distorted from an ideal 90 ° and 270° (based upon a pure delocalization argument), which presumably lies in the fact that the sterics of the peripheral amide groups have an effect on the precise position of the maxima on the potential energy surface. Interestingly, the ground state structure with a dihedral of *ca.* 180° was found to be highly dependent on the method used in the calculations. This particular conformation brings the pyrene and quinoline rings into close proximity; in these calculations we included dispersion effects into the method (DFT-D) in order to satisfactorily account for weak non-bonding interactions in this relatively sterically hindered system. The structures thereby obtained exhibit an angle between the two planes of 13°, whereas calculations performed without considering dispersion effects gave an analogous structure with an angle of 73°. Whilst the addition of dispersion effects gave only modest differences to the relative energies of the two ground state structures was largely unaffected (within typical error limits assigned to DFT calculations), it is clear that the addition of such corrections can have a significant effect on the conformation of calculated structures, and highlights the potential for dispersion effects to increase the accuracy and reliability of structural prediction and interpretation.[20]

The two ground state isomers are calculated to be within 2 kJ.mol^{-1}, which is essentially isoenergetic within typical DFT error limits. This is entirely consistent with the isomers being present in approximately equal concentrations, as determined by NMR spectroscopy. Moreover, the calculated activation barriers for interconversion of the isomers give ΔG = 102 and 107 kJ.mol^{-1}, which are relatively high; given that no interconversion was detected by NMR spectroscopy at room temperature, these calculated activation energies are consistent with the experimental observations. These results can be favourably compared to a study in which the rotation of an N-aryl bond was investigated.[21] The activation barrier was found to be *ca.* 77 kJ.mol^{-1}, and rotation of the aryl group was observed only upon heating to ≥ 70 °C; given that no such interchange was observed for the system described here, the calculated values are plausible and support the experimental data. Coordinates for the calculated structures are provided in the ESI.

Synthesis and characterization of cyclometalated Pt(II) complexes

The target complexes [Pt(**L$^{1-4}$**)(acac)] were synthesised in two steps from K_2PtCl_4 *via* the precursor [(**L**)Pt-μ-Cl$_2$Pt(**L**)] dimer (obtained *via* dropwise addition of K_2PtCl_4 in water to the ligand in 2-ethoxyethanol).[22] The resultant dimers were split by DMSO[23] to give the intermediate monometallic DMSO adduct [Pt(**L**)(DMSO)Cl] which was then reacted with sodium acetylacetonate to give [Pt(**L$^{1-4}$**)(acac)].

For [Pt(**L^3**)(acac)], ^{1}H NMR spectroscopy showed (SI, Fig. S2) a single isomer consistent with the **HL^3** data, with a single set of proton resonances associated with the coordinated β-diketonate ligand (one bridging C*H* resonance *ca.* 5.5 ppm, and two unique methyl resonances *ca.* 2 ppm due to the unsymmetrical nature of the Pt coordination sphere) and the diastereotopic methylene protons again at 5.5 - 6.5 ppm. In comparison [Pt(**L^2**)(acac)] and [Pt(**L^4**)(acac)] revealed more complex ^{1}H NMR spectra, with the presence of two isomers giving overlapping aromatic resonances

due to doubling of the signals. For these speices, the aliphatic region was more informative, as indicated *via* resonances of the coordinated β-diketonate ligand (two singlets at *ca.* 5.5 ppm that correspond to the bridging C*H*, and four singlets around 2 ppm assigned to the methyl groups), and the two sets of diastereotopic protons for the methylene group at 4.5-6.5 ppm that are subtly shifted from the free ligands. Variable temperature NMR spectroscopy revealed no interchange of the isomers at elevated temperatures (up to 90°C in d_8-toluene), which correlates with the high activation barrier for isomerisation predicted by the computational studies on **HL**[4]. The downfield region of the $^{13}C\{^1H\}$ NMR spectra (SI, Figs S3 and S4) for the complexes was also informative revealing two resonances >180 ppm for the coordinated acac ligand in both [Pt(**L**[1])(acac)] and [Pt(**L**[3])(acac)], but four resonances for [Pt(**L**[2])(acac)] and [Pt(**L**[4])(acac)], again consistent with the presence of two isomeric forms in the latter complexes. The large number of unique aromatic resonances in [Pt(**L**[3])(acac)] (SI, Fig S4) was anticipated for a rigid ligand system with restricted rotation about the amide functional group.

The $^{195}Pt\{^1H\}$ NMR spectra (for example, SI, Fig S5) for the complexes revealed little variation according to ligand type with broad resonances of δ_{Pt} -2776 [Pt(**L**[1])(acac)], -2784 [Pt(**L**[2])(acac)], -2786 [Pt(**L**[3])(acac)] and -2788 ppm [Pt(**L**[4])(acac)] which are consistent with our previous data on cyclometalated Pt(II) complexes[17] that incorporate the 2-phenylquinoline chelate, as well as comparable with the value of δ_{Pt} -2868 ppm for [Pt(ppy)(acac)] (where ppy = 2-phenylquinoline).[24] The similarities in the values suggest that the donating ability of the cyclometalating ligand essentially remains unchanged by the variation in the chromophoric component of the ligand backbone.

X-ray crystal structure determinations

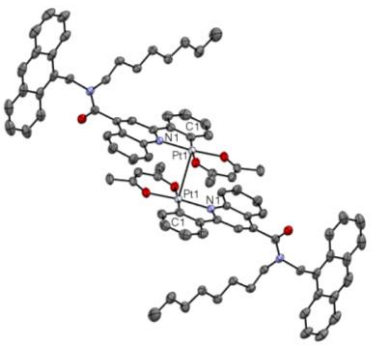

Figure 2. X-ray crystal structure of [Pt(**L**[3])(acac)]. Hydrogen atoms are omitted for clarity and ellipsoids are drawn at 50% probability.

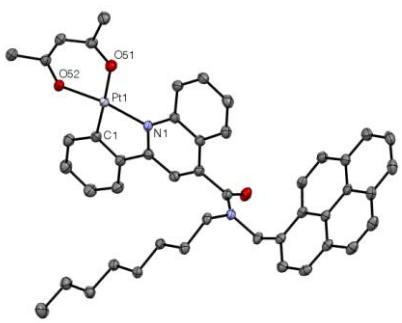

Figure 3. X-ray crystal structure of [Pt(**L**[4])(acac)]. Hydrogen atoms are omitted for clarity and ellipsoids are drawn at 50% probability.

Table 1. Data collection parameters for the X-ray structures.

Crystal	[Pt(L[3])(acac)]	[Pt(L[4])(acac)]
Empirical Formula	$C_{44}H_{44}N_2O_3Pt$	$C_{49.5}H_{48}N_2O_3Pt$
Formula wt / g mol^{-1}	843.90	913.99
Crystal System, space group	Monoclinic, *P2$_1$/c*	Triclinic, *P-1*
a/Å	17.5181(11)	8.9153(5)
b/Å	14.2716(10)	12.6111(9)
c/Å	16.0586(11)	18.5893(13)
α/°	90	77.279(3)
β/°	117.1440(5)	83.655(3)
γ/°	90	76.145(3)
Vol/Å^3	3572.6(4)	1975.7(2)
Z, Calc density (Mgm^{-3})	4, 1.569	2, 1.536
Abs coeff (mm^{-1})	3.971	3.597
F(000)	1696	922
Crystal	Red plate	Orange plate
Crystal Dimensions/ mm^3	0.09 × 0.06 × 0.01	0.24 × 0.14 × 0.02
θ range (°)	2.613 – 27.505	2.533 – 27.521
No. of reflections collected	62763	26820
R_{int}	0.0502	0.0484
Max. and min. transmission	1.000 and 0.819	1.000 and 0.642
No. of data/restraints/ parameters	8196 / 0 / 454	9045 / 80 / 536
Goodness-of-fit on F^2	1.045	1.048
Final *R* indices [$F^2 > 2\sigma(F^2)$]: R_1, wR_2	0.0236, 0.0592	0.0303, 0.0843
R indices (all data) : R_1, wR_2	0.0264, 0.0611	0.0313, 0.0853
Largest diff. peak and hole/e Å^{-3}	1.589, -0.578	1.697, -1.339

Crystals suitable for X-ray diffraction studies were isolated by slow evaporation of concentrated $CHCl_3$ solutions of complex. Pleasingly two structures confirmed the proposed formulations for the complexes [Pt(**L**[3])(acac)] and [Pt(**L**[4])(acac)]. Data collection parameters are shown in Table 1 and selected bond lengths (Å) and angles (°) are in Table 2.

The structure of [Pt(**L**[3])(acac)] has comparable coordination sphere bond lengths to those reported for [Pt(ppy)(acac)].[25] The anthracenyl moiety is almost perpendicular to the plane of the phenylquinoline unit (104.86(8)°), providing organised packing. This head-to-tail arrangement results in both *π-π* (of the phenylquinoline units) and Pt-Pt interactions, with a formal Pt-Pt bond length of 3.2365(2) Å in the solid state. This compares to a distance of *ca.* 3.7 Å for a Pt-Pt interaction in the reported structure of [Pt(ppy)(acac)].[33]

In contrast, the structure of [Pt(**L**^{4})(acac)] revealed an isomer which positions the pyrene unit away from the phenylquinoline. The packing arrangement results in very little π-stacking interactions between the phenylquinoline units and, somewhat surprisingly, none between the pyrene moieties. However, this could be due to the positioning of the octyl chain, which can be seen lying between the pyrene units. There was no evidence for metallophilic interactions in [Pt(**L**^{4})(acac)], presumably due to the bulk of the ligand preventing such interactions in the crystalline form.

It is noteworthy that, with reference to the DFT calculations on the conformational aspects of **HL**^{4}, both X-ray structural studies reveal arrangements of the ligand where the chromophore was positioned away from the phenylquinoline unit and is not stacking. In the case of [Pt(**L**^{3})(acac)], supporting spectroscopic data has already shown that the species exists as a single isomer, the precise conformational nature of which has been structurally identified by the X-ray studies above. However, for [Pt(**L**^{4})(acac)] the NMR studies showed that two isomers, as supported by the computational work, co-exist, although only one of these isomers was isolated through crystallisation.

Table 2. Selected bond lengths (Å) and bond angles (°) from the crystallographic data.

[Pt(**L**^{3})(acac)]		[Pt(**L**^{4})(acac)]	
Bond lengths (Å)			
Pt(1)-C(1)	1.962(3)	Pt(1)-C(1)	1.970(3)
Pt(1)-O(51)	2.0032(17)	Pt(1)-O(52)	1.998(2)
Pt(1)-N(1)	2.0550(18)	Pt(1)-N(1)	2.056(3)
Pt(1)-O(52)	2.1057(18)	Pt(1)-O(51)	2.098(2)
Pt(1)-Pt(1)′	3.2365(2)		
Bond angles (°)			
C(1)-Pt(1)-O(51)	89.21(9)	C(1)-Pt(1)-O(52)	89.44(11)
C(1)-Pt(1)-N(1)	80.83(9)	C(1)-Pt(1)-N(1)	81.28(12)
O(51)-Pt(1)-N(1)	169.91(8)	O(52)-Pt(1)-N(1)	170.39(9)
C(1)-Pt(1)-O(52)	174.64(8)	C(1)-Pt(1)-O(51)	177.52(9)
O(51)-Pt(1)-O(52)	88.17(7)	O(52)-Pt(1)-O(51)	89.07(9)
N(1)-Pt(1)-O(52)	101.63(7)	N(1)-Pt(1)-O(51)	100.11(10)

UV-vis. and luminescence spectroscopy

The free ligands exhibit absorption bands assigned to the different, and overlapping, ligand-centred (LC) $^1\pi\rightarrow\pi^*$ transitions of the 2-phenylquinoline and the appended chromophores. For **HL**^{2} the 2-phenylquinoline and naphthyl bands overlap in the range 250-350 nm. For **HL**^{3} and **HL**^{4} the longer wavelength absorptions of the anthracene and pyrene chromophores were clearly assigned due to the distinctive vibronic character of these bands between 320-400 nm (Fig. 4). In particular, the spectrum of **HL**^{4} is a classical representation of a pyrene absorption with the three vibronic bands clearly visible at 345, 329 and 316 nm. For **HL**^{4}, supporting TD-DFT calculations were employed to corroborate the nature of the observed electronic transitions and consider the potential influence of the two non-interchangeable isomeric forms (see earlier discussion on the conformational analysis of **HL**^{4}). The simulated spectra (see ESI) for the two isomers (assuming O-C-N-C_{pyrene} dihedral angles of 0 and 180°) showed little difference in the position of the wavelength maxima, with only slight variation in oscillator strengths for the major transitions. The calculations have allowed confirmation of the expected π-π^* character to the transitions. However, it would be inappropriate to closely compare the experimental and calculated spectra since the former will comprise a superimposition of the absorption spectra of both isomers.

For the Pt(II) complexes the presence of ligand-centred transitions remain. For all complexes there was an additional broad band at lower energy (*ca.* 400-480 nm) assigned to a ^{1}MLCT ($5d\rightarrow\pi^*$) transition. Our previous studies have employed TD-DFT to elucidate the nature of the lowest energy absorption of substituted 2-phenylquinoline [Pt(L)(acac)] complexes, showing that there is a strong MLCT component (*i.e.* significant *d*-orbital parentage to the HOMO) to this band (ESI, Scheme S1).[17] Both [Pt(**L**^{3})(acac)] and [Pt(**L**^{4})(acac)] also showed the expected vibronic structure attributed to the anthracene and pyrene chromophores (in these cases the positions of the pyrene-based vibronic bands are unaltered when compared to the free ligands), respectively, the tail of which overlaps with the ^{1}MLCT band (Fig. 4). In the luminescence studies, firstly, the free ligands were found to be fluorescent in solution, and in the case of **HL**^{2}-**HL**^{4} the emission profiles were dominated by the appended fluorophore in each case (for example, see SI, Fig S6). **HL**^{3} gave a characteristic structured emission profile associated with the anthracene fluorophore, whilst **HL**^{4} revealed two peaks at 395 and 438 nm, which is consistent with excimer type fluorescence. All emission lifetimes for the ligands were < 10ns and consistent with an emitting state of $^1\pi$-π^* character.

The luminescence from [Pt(**L**^{1})(acac)], which does not incorporate an additional chromophore, was dominated by a broad, featureless emission maximum at 618 nm assigned to a ^{3}MLCT excited state; the corresponding excitation spectrum was dominated by MLCT bands around 425 nm. The emission character of [Pt(**L**^{1})(acac)] was sensitive to dissolved oxygen: the intensity of the ^{3}MLCT band increased upon degassing of the solvent, whilst the observed lifetime extended from 380 ns (aerated) to 3.4 μs (degassing). A wide range of luminescent complexes have previously shown varying sensitivity to dissolved oxygen, including a number of cyclometalated Pt(II) species.[9]

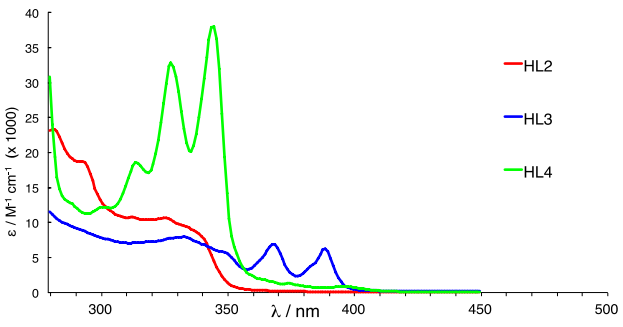

Figure 4. UV-vis. absorption spectra for selected ligands ($CHCl_3$).

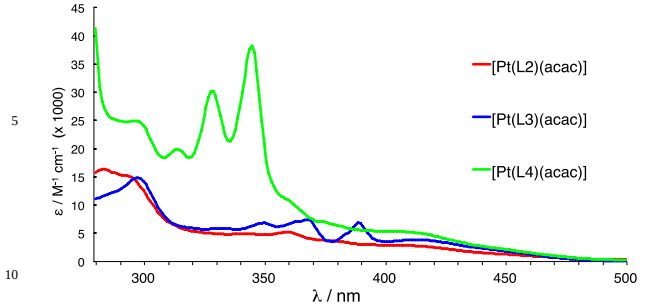

Figure 5. UV-vis. absorption spectra for selected Pt(II) complexes ($CHCl_3$).

In contrast to [Pt(**L**^{1})(acac)], the room temperature emission profiles of the chromophore-appended complexes [Pt(**L**$^{2\text{-}4}$)(acac)] in aerated chloroform revealed two main components: (i) a chromophore-centred fluorescence <500 nm (with corresponding lifetimes consistent with $^1\pi$-π* character); (ii) a broad featureless band at *ca.* 605 nm attributed to a metal-based excited state of strong ^{3}MLCT character (*e.g.* Fig. 6). These complexes can therefore be described as dual emissive (Table 3). The excitation profiles (λ_{em} 605 nm) for [Pt(**L**^{2})(acac)], [Pt(**L**^{3})(acac)] and [Pt(**L**^{4})(acac)] all exhibited the MLCT band common to each complex around 420 nm, as well as bands that could be clearly assigned to naphthyl, anthracenyl or pyrenyl-centred transitions, respectively, all <400 nm. Room temperature degassed measurements on [Pt(**L**$^{2\text{-}4}$)(acac)] showed an increase in the integrated intensity of the ^{3}MLCT emission band, again suggesting a sensitivity to $^3O_2$ quenching (Fig. 6).

Lifetime measurements (SI, Fig S7) on [Pt(**L**$^{2\text{-}4}$)(acac)] (Table 3) in aerated solvent lie in the range 258-543 ns (*cf.* [Pt(**L**^{1})(acac)] with τ = 380 ns) and showed varied sensitivity to solvent degassing. For [Pt(**L**^{2})(acac)] the lifetime of the ^{3}MLCT state in chloroform was 543 ns, which extended to 6.6 μs under degassing. Under the same conditions, the properties of the anthracenyl derivative [Pt(**L**^{3})(acac)] were similar to [Pt(**L**^{1})(acac)] (2.9 μs *vs* 3.4 μs). In comparison [Pt(**L**^{4})(acac)], which possessed the shortest aerated ^{3}MLCT lifetime of 258 ns, revealed a remarkable extension in this lifetime to 42.0 μs when measured under degassed conditions (SI, Fig. S7).

The potential interplay of the ^{3}LC states of the appended chromophore (naphthyl, anthracenyl or pyrenyl) and ^{3}MLCT excited states was investigated using low temperature (77K)

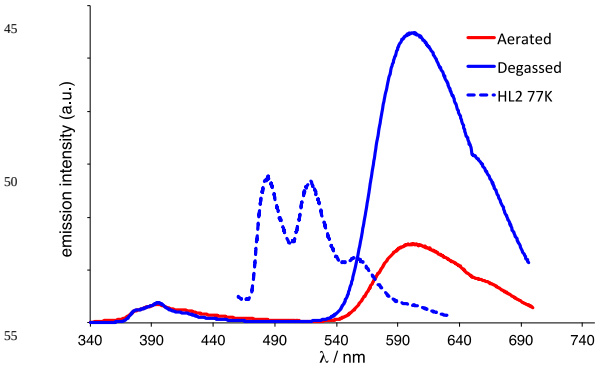

Figure 6. Comparison of the room temperature emission spectra of [Pt(**L**^{2})(acac)] in aerated (red line) and degassed chloroform (blue line). The low temperature emission spectrum of **HL**^{2} (blue dashed line) as a glass (EtOH:$CHCl_3$, 1:1) is shown for comparison.

measurements on glasses (EtOH:$CHCl_3$, 1:1) of the corresponding ligands. For example, Figure 6 shows that the vibronically structured triplet emission from the naphthyl moiety ($^3LC_{nap}$) for **HL**^{2}, with an onset *ca.* 21300 cm^{-1} lies well above, and with minimal overlap of, the ^{3}MLCT state of [Pt(**L**^{2})(acac)], which peaks at *ca.* 16600 cm^{-1}.

Analogous measurements for [Pt(**L**^{4})(acac)] reveal (Figure 7) typical emission from the triplet state of pyrene ($^3LC_{pyr}$) peaking at *ca.* 16700 cm^{-1}, which is in agreement with previous literature reports.[11] Figure 7 clearly shows that there is significant spectral overlap of the $^3LC_{pyr}$ and ^{3}MLCT (peaking at *ca.* 16600 cm^{-1}) bands in [Pt(**L**^{4})(acac)] and suggests that the energy matching of these two states could lie within <500 cm^{-1}. The dramatic increase in ^{3}MLCT lifetime of [Pt(**L**^{4})(acac)] under degassed conditions suggests that interplay between the two states *via* through-space energy transfer may result in the thermal equilibration of the ^{3}MLCT and $^3LC_{pyr}$ states. The good energy matching of the triplet levels of the complex and pyrene chromophore can allow thermal equilibration under degassed solvent conditions, giving rise to the energy reservoir effect whereby the ^{3}MLCT lifetime is extended by the long-lived $^3LC_{pyr}$ state (see SI, Scheme S2).[11] Conversely, under aerated conditions the relatively shortened ^{3}MLCT lifetime of [Pt(**L**^{4})(acac)] *versus*

Table 3. Electronic spectroscopic data for the complexes.

Compound	λ_{abs} [a] / nm	λ_{em} [a,b] / nm	τ [a,c] / ns	τ [a,d] / ns	τ [e] / μs	λ_{em} [f] / nm	Φ [g]
			293K (aerated)		293K (degassed)	77K	
[Pt(L^1)(acac)]	300, 349, 368, 417	618	-	380	3.4	-	0.006
[Pt(L^2)(acac)]	261, 273, 284, 294, 342, 359, 378, 406	603	< 1 (1.1)	543	6.6	485, 520, 571	0.021
[Pt(L^3)(acac)]	257, 298, 350, 362, 368, 389, 413	606	3.3 (1.9)	356	2.9	453, 488, 529, 578	0.007
[Pt(L^4)(acac)]	256, 266, 278, 297, 314, 329, 345, 361, 408	603	3.9 (2.8, 7.2)	258	42.0 (95%), 3.7 (5%)	601, 616, 652, 666	0.005

[a] at 293 K, in aerated chloroform; [b] ^{3}MLCT emission (excited using 350 or 420 nm); [c] ligand-centred fluorescence lifetime (295 or 372 nm) with corresponding free ligand values in parentheses; [d] ^{3}MLCT lifetime (excited using 372 or 459 nm); [e] ^{3}MLCT lifetime in chloroform (excited using 355 nm); [f] in ethanol/chloroform (1:1) glass at 77K, excited using 350 or 420 nm; [g] quantum yield obtained in aerated chloroform, using $[Ru(bipy)_3](PF_6)_2$ in aerated MeCN as a standard (Φ = 0.016).[26]

[Pt(**L**^{1})(acac)] may be due to ^{3}MLCT→^{3}LC$_{pyr}$ energy transfer that provides a quenching pathway due to efficient deactivation of the ^{3}LC$_{pyr}$ by dissolved ^{3}O$_2$.

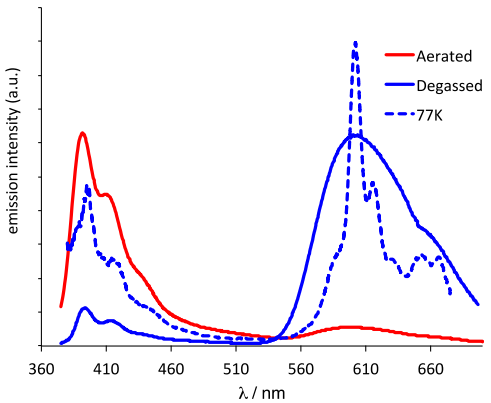

Figure 7. Comparison of the room temperature emission spectra of [Pt(**L**^{4})(acac)] in aerated (red line), degassed chloroform (blue line) with the low temperature (blue dashed line) emission spectrum (EtOH:CHCl$_3$, 1:1).

In contrast to [Pt(**L**^{4})(acac)], the luminescence data for [Pt(**L**^{3})(acac)] suggests that no energy reservoir effect was in operation. In literature reports, the triplet excited state of anthracene (^{3}LC$_{anth}$) has been observed around 14500 cm^{-1}.[27] However, in the context of the work herein, luminescence data for 9-(methylaminomethyl)anthracene, as reported by de Melo *et al.*,[28] is much more structurally relevant to the chromophore represented in [Pt(**L**^{3})(acac)]. Low temperature measurements on [Pt(**L**^{3})(acac)] (and **HL**^{3}) suggest that the ^{3}LC$_{anth}$ state of this anthracenyl chromophore is significantly higher in energy than that known for anthracene, with an onset *ca.* 22200 cm^{-1}; this is consistent with the previously reported observations for 9-(methylaminomethyl)anthracene.[36] Therefore, for [Pt(**L**^{3})(acac)] it is likely that the ^{3}LC$_{anth}$ excited state lies well above the ^{3}MLCT state (SI, Scheme S2). This results in poor energy matching of the excited states, yielding ^{3}MLCT characteristics which are comparable to the non-chromophoric analogue [Pt(**L**^{1})(acac)].

In summary, this paper has described the synthetic pathway to lipophilic, chromophore functionalised cyclometalated Pt(II) complexes. These new species have been characterised using a range of spectroscopic and analytical techniques, and two examples have been structurally characterised in the solid state using single crystal X-ray diffraction. Luminescence studies have shown that for the chromophore functionalised complexes dual emission is apparent, with both ligand-based fluorescence and Pt(II)-based ^{3}MLCT phosphorescence observed. The intensity of the ^{3}MLCT emission was found to be sensitive to dissolved oxygen. In the case of the pyrene-appended complex [Pt(**L**^{4})(acac)] degassing led to a dramatic elongation of the ^{3}MLCT lifetime, which was attributed to good energetic matching with the pyrene-based triplet state and an energy reservoir effect. For the naphthyl and anthracenyl variants the ligand-based triplet states lie well above the level of the ^{3}MLCT state and therefore do not show the same effect.

Experimental Section

X-ray crystallography

Suitable crystals were selected and measured following a standard method[29] on a *Rigaku AFC12* goniometer equipped with an enhanced sensitivity (HG) *Saturn724+* detector mounted at the window of a *FR-E+ SuperBright* molybdenum rotating anode generator with either VHF *Varimax* optics (70µm focus) ([Pt(**L**^{3})(acac)]) or HF *Varimax* optics (100µm focus) ([Pt(**L**^{4})(acac)]) at 100K. Cell determination, data collection, reduction, cell refinement and absorption correction carried out using *CrystalClear-SM Expert 3.1b27*.[30]

The structures were solved by charge flipping using *SUPERFLIP*[31] and were completed by iterative cycles of ΔF-syntheses and full-matrix least squares refinement. All non-H atoms were refined anisotropically and difference Fourier syntheses were employed in positioning idealized hydrogen atoms and were allowed to ride on their parent C-atoms. Disordered solvent molecules were modelled using partial occupancy. All refinements were against F^2 and used *SHELXL-2014*.[32] Figures were created using the ORTEP3 software package. CCDC reference numbers 1443584 [Pt(**L**^{3})(acac)] and 1443585 [Pt(**L**^{4})(acac)], contain the supplementary crystallographic data for this paper. These data can be obtained free of charge from the Cambridge Crystallographic Data Centre *via* www.ccdc.cam.ac.uk/data_request/cif.

DFT Calculations

All calculations were performed on the Gaussian 09 suite.[33] Relaxed potential energy scans were calculated by fixing the O–C–N–C$_{pyrene}$ dihedral angle, and allowing the structure to optimize at each value of the scanned parameter. The structures corresponding to the minima and maxima of the potential energy surface were thereafter used as a starting geometry for a subsequent transition state calculation. Molecular geometries were optimized without restraints, and were followed by frequency calculations to ascertain the nature of the stationary point (minimum *vs.* saddle point). Frequency calculations of transition state structures showed only a single imaginary frequency, corresponding to the expected reaction coordinate. Calculations were performed using the restricted B3LYP hybrid functional,[34] incorporating the D3 version of Grimme's dispersion correction.[35] The 6-31G(d,p) double ζ basis set was used for all centres.[36] Coordinates of all optimized structures are provided in the supplementary material. TD-DFT calculations were performed using the unrestricted B3LYP functional employing 6-31+G(d,p) basis set on all centres. The first 24 excited states were calculated; details of those excited states are provided in the ESI.

General

^{1}H and ^{13}C{^{1}H} NMR spectra were run on NMR-FT Bruker 250 or 400 spectrometers, ^{195}Pt{^{1}H} on NMR-FT 500 spectrometer (all recorded in CDCl$_3$). ^{1}H and ^{13}C{^{1}H} NMR chemical shifts (δ) were determined relative to internal TMS and are given in ppm. Low-resolution mass spectra were obtained by the staff at Cardiff

University. High-resolution mass spectra were carried out by at the EPSRC National Mass Spectrometry Service at Swansea University. UV-Vis studies were performed on a Jasco V-570 spectrophotometer as chloroform solutions. Photophysical data were obtained on a JobinYvon-Horiba Fluorolog spectrometer fitted with a JY TBX picosecond photodetection module and a Hamamatsu R5509-73 detector (cooled to -80°C using a C9940 housing). Emission spectra were uncorrected and excitation spectra were instrument corrected. The pulsed sources were either a Nano-LED configured for 372 nm or 459 nm output (operating at 500 kHz) or a Continuum Minilite Nd:YAG laser at 355 nm (operating at 15 Hz). Degassed samples were prepared by a thricely freeze-pump-thaw treatment of solutions using a bespoke cell fitted with a Young's tap and solvent bulb. Luminescence lifetime profiles were obtained using the JobinYvon-Horiba FluoroHub single photon counting module and the data fits yielded the lifetime values using the provided DAS6 deconvolution software.

Materials

All reactions were performed with the use of vacuum line and Schlenk techniques. Reagents were commercial grade and were used without further purification. 2-phenyl-4-quinolinecarboxylic acid and potassium tetrachloroplatinate were used as purchased from Alfa Aesar.

General synthesis for P^{2-4}.

Equimolar aryl aldehyde and 1-octylamine were dissolved in ethanol (20 mL) and heated at reflux for 16 h under dinitrogen. The reaction was cooled and $NaBH_4$ (excess) was added in portions. The reaction was stirred for a further 16 h before dilution with dichloromethane (20 mL) and then washed with water (2 × 20 mL) and brine (20 mL). The organic phase was dried over $MgSO_4$ before the solvent was removed *in vacuo*.

Synthesis of P^2: using 1-naphthaldehyde (0.254 g, 1.628 mmol), 1-octylamine (0.210 g, 1.628 mmol) and $NaBH_4$ (0.124 g, 3.256 mmol). The product was obtained as a light yellow oil. Yield = 0.358 g (82%). ^{1}H NMR (400 MHz, $CDCl_3$): δ_H 8.04 (1H, d, $^3J_{HH}$ = 8.0 Hz), 7.85 (1H, dd, J_{HH} = 8.0, 1.6 Hz), 7.77 (1H, dd, J_{HH} = 7.6, 1.6 Hz), 7.54 – 7.39 (4H, m), 4.21 (2H, s), 2.70 (2H, t, $^3J_{HH}$ = 7.2 Hz), 1.56 – 1.49 (2H, m), 1.33 – 1.19 (10H, m), 0.86 (3H, t, $^3J_{HH}$ = 7.2 Hz) ppm.

Synthesis of P^3: using 9-anthraldehyde (0.163 g, 0.789 mmol), 1-octylamine (0.102 g, 0.789 mmol) and $NaBH_4$ (0.060 g, 1.577 mmol. The product was purified by column chromatography (silica) and was eluted with dichloromethane/methanol (9:1). Yield = 0.242 g (96%). ^{1}H NMR (400 MHz, $CDCl_3$): δ_H 8.41 (1H, s), 8.34 (2H, dd, J_{HH} = 8.8 Hz, 0.8 Hz), 8.01 (2H, d, $^3J_{HH}$ = 8.4 Hz), 7.54 (2H, dd, J_{HH} = 8.8 Hz, 6.4, 1.2 Hz), 7.48-7.46 (2H, m), 4.73 (2H, s), 2.87 (2H, t, $^3J_{HH}$ = 7.2 Hz), 1.62 – 1.55 (2H, m), 1.35 – 1.23 (10H, m), 0.88 (3H, t, $^3J_{HH}$ = 1.6 Hz) ppm.

Synthesis of P^4: using 1-pyrenecarboxaldehyde (0.169 g, 0.733 mmol), 1-octylamine (0.095 g, 0.733 mmol) and $NaBH_4$ (0.056 g, 1.466 mmol). The product was purified by column chromatography (silica) and was eluted with dichloromethane/methanol (9:1). Yield = 0.246 g (98%). ^{1}H NMR (400 MHz, $CDCl_3$): δ_H 8.35 (1H, d, $^3J_{HH}$ = 9.2 Hz), 8.20 – 8.16 (2H, m), 8.15 – 8.12 (2H, m), 8.04 – 7.98 (4H, m), 4.49 (2H, s), 2.79 (2H, t, $^3J_{HH}$ = 7.2 Hz), 1.62 – 1.54 (2H, m), 1.35 – 1.22 (10H, m), 0.88 (3H, t, $^3J_{HH}$ = 6.8 Hz) ppm. ^{13}C{^{1}H} NMR (125.8 MHz, $CDCl_3$): δ_C 131.3, 130.9, 130.8, 129.2, 127.9, 127.5, 127.4, 127.4, 127.3, 125.9, 125.2, 125.1, 124.7, 122.9, 50.9, 49.3, 31.8, 29.4, 29.3, 29.2, 27.3, 22.6, 14.1 ppm. MS(ES) found *m/z* = 344.2 $[M + H]^+$. UV-vis ($CHCl_3$): λ_{max} (ε / dm^3 mol^{-1} cm^{-1}) 266 (23400), 277 (39600), 300 (4720), 314 (11400), 327 (26700), 344 (39000) nm. IR (thin film): ν_{max} 3040, 2953, 2928, 2855, 2816, 1603, 1587, 1458, 1443, 1184, 1096, 841, 802, 710 cm^{-1}.

General method for the synthesis of the ligands[37]

Thionyl chloride (excess) was added, dropwise, to a stirring suspension of 2-phenyl-4-quinolinecarboxylic acid (1.1 eq.) in chloroform (10 mL). The reaction was heated at reflux for 16 h under dinitrogen. The solvent was removed *in vacuo* and the yellow solid, 2-phenyl-4-quinolinecarbonyl chloride, redissolved in chloroform (10 mL) before the amine (1 eq.) was added slowly to the stirring solution. EtN^iPr_2 (excess) was added dropwise and the mixture was stirred for 16 h at room temperature under dinitrogen. The solvent was removed *in vacuo* before being redissolved in dichloromethane (20 mL). The crude mixture was washed with $NaHCO_3$ (sat. sol., 2 × 20 mL), water (1 × 20 mL) and brine (1 × 20 mL). The organic phase was dried over $MgSO_4$ and filtered before the solvent was removed *in vacuo*.

Synthesis of HL^1: using 2-phenyl-4-quinolinecarboxylic acid (0.465 g, 1.869 mmol) and 1-octylamine (0.219 g, 1.699 mmol). Yield = 0.434 g (71%). ^{1}H NMR (400 MHz, $CDCl_3$): δ_H 7.98 (1H, d, $^3J_{HH}$ = 8.4 Hz), 7.94 - 7.91 (2H, m), 7.84 (1H, d, $^3J_{HH}$ = 8.0 Hz), 7.60 – 7.56 (1H, m), 7.51 (1H, s), 7.42 - 7.40 (3H, m), 7.33 – 7.29 (1H, m), 6.93 (1H, br. t, $^3J_{HH}$ = 4.4 Hz), 3.35 - 3.30 (2H, m), 1.59 – 1.52 (2H, m), 1.34 – 1.19 (10H, m), 0.90 (3H, t, $^3J_{HH}$ = 6.4 Hz) ppm. ^{13}C{^{1}H} NMR (75.6 MHz, $CDCl_3$): δ_C 167.6, 156.7, 148.5, 143.4, 138.7, 130.3, 129.9, 129.0, 127.5, 127.3, 125.1, 123.4, 116.4, 40.3, 31.9, 29.7, 29.4, 27.1, 22.8, 14.2 ppm. MS (ES) found *m/z* = 361.22 $[M + H]^+$. UV-vis (ε / M^{-1} cm^{-1}) ($CHCl_3$) λ_{max}: 263 (29100), 327 (6610) nm. IR ν_{max} (thin film): 3306 (N-H), 1636 (C=O) cm^{-1}.

Synthesis of HL^2: using 2-phenyl-4-quinolinecarboxylic acid (0.235 g, 0.941 mmol) and P^2 (0.231 g, 0.855 mmol. Yield = 0.268 g (89%). ^{1}H NMR (400 MHz, $CDCl_3$): *major isomer* δ_H 8.42 (1H, d, $^3J_{HH}$ = 8.4 Hz), 8.19 – 7.32 (16H, m), 5.72 (1H, d, $^2J_{HH}$ = 14.4 Hz, C*H*H), 5.18 (1H, d, $^2J_{HH}$ = 14.4 Hz, CH*H*), 2.94 – 2.80 (2H, m), 1.47 – 0.86 (12H, m), 0.79 (3H, t, $^3J_{HH}$ = 6.8 Hz) ppm; *minor isomer* δ_H 8.19 – 7.32 (17H, m), 4.92 – 4.72 (2H, br. m), 2.94 – 2.80 (2H, m), 1.92 – 1.79 (2H, br. m), 1.47 – 0.86 (13H, m) ppm. ^{13}C{^{1}H} NMR (125.8 MHz, $CDCl_3$): *Both isomers* δ_C 167.7, 155.8, 147.4, 142.7, 138.1, 130.5, 130.4, 129.2, 129.1, 128.6, 128.5, 127.9, 127.7, 126.4, 126.4, 126.1, 125.8, 124.3, 123.7, 123.1, 122.2, 114.9, 45.7, 38.0, 30.4, 28.1, 27.6, 27.4, 25.2, 21.4, 13.0 ppm. HR-MS: calcd. 501.2900 for $[C_{35}H_{37}N_2O]^+$, found *m/z* = 501.2889. UV-vis ($CHCl_3$): λ_{max} (ε / dm^3 mol^{-1} cm^{-1}) 263 (46500), 282 (19400), 293 (15600), 312 (8980), 325 (8880), 336 (7570) nm. IR (thin film): ν_{max} 3059, 2926, 2853, 1638, 1597, 1549, 1510, 1466, 1460, 1406, 1377, 1348, 1248, 1028, 793, 772, 760, 741, 694, 665 cm^{-1}.

Synthesis of HL[3]: using 2-phenyl-4-quinolinecarboxylic acid (0.163 g, 0.656 mmol) and P[3] (0.190 g, 0.596 mmol). Yield = 0.282 g (86%). ^{1}H NMR (400 MHz, $CDCl_3$): δ_H 8.58 – 8.54 (3H, m), 8.17 – 8.08 (5H, m), 7.84 (1H, s), 7.80 (1H, d, $^3J_{HH}$ = 7.2 Hz), 7.71 – 7.65 (3H, m), 7.58 – 7.46 (5H, m), 7.39 (1H, m), 6.28 (1H, d, $^2J_{HH}$ = 15.2 Hz, C*H*H), 5.82 (1H, d, $^2J_{HH}$ = 15.2 Hz, CH*H*), 2.51 (2H, app. t), 1.39 – 1.25 (2H, br m), 1.08 – 0.53 (13H, overlapping m) ppm. ^{13}C{^{1}H} NMR (125.8 MHz, d_6-DMSO): δ_C 167.7, 155.8, 147.4, 142.7, 138.1, 130.5, 130.4, 130.2, 129.2, 129.1, 128.6, 128.5, 128.0, 127.9, 127.7, 126.6, 126.4, 126.4, 126.2, 126.1, 125.8, 125.6, 124.3, 124.0, 123.7, 123.1, 122.2, 114.9, 45.7, 38.0, 30.6, 30.4, 28.1, 27.9, 27.8, 27.6, 27.4, 26.9, 25.8, 25.2, 21.5, 21.4, 13.1, 12.9 ppm. HR-MS: calcd. 551.3057 for $[C_{39}H_{39}N_2O]^+$, found *m/z* = 551.3051. UV-vis ($CHCl_3$): λ_{max} (ε / dm^3 mol^{-1} cm^{-1}) 258 (55700), 333 (7980), 350 (5680), 368 (6960), 389 (6320) nm. IR (thin film): ν_{max} 3057, 2955, 2924, 2855, 1628, 1593, 1549, 1495, 1462, 1447, 1431, 1406, 1373, 1343, 1263, 1240, 1180, 1159, 1123, 1028, 889, 767, 759 cm^{-1}.

Synthesis of HL[4]: using 2-phenyl-4-quinolinecarboxylic acid (0.235 g, 0.941 mmol) and P[4] (0.231 g, 0.855 mmol). Yield = 0.268 g, (89%). ^{1}H NMR (400 MHz, $CDCl_3$): *major isomer* δ_H 8.55 (1H, d, $^3J_{HH}$ = 8.0 Hz), 8.22 – 7.05 (18H, m), 5.92 (1H, d, $^2J_{HH}$ = 14.5 Hz, C*H*H), 5.18 (1H, d, $^2J_{HH}$ = 14.4 Hz, CH*H*), 2.76 (2H, app. q), 1.92 – 0.86 (12H, m), 0.66 (3H, t, $^3J_{HH}$ = 6.8 Hz) ppm; *minor isomer* δ_H 8.22 – 7.05 (19H, m), 4.92 – 4.72 (2H, br. app. q), 4.31 – 4.11 (1H, br. s), 3.38 – 3.16 (1H, br. s), 1.92 – 0.72 (15H, overlapping m) ppm. HR-MS: calcd. 575.3057 for $[C_{41}H_{39}N_2O]^+$, found *m/z* = 575.3046. UV-vis ($CHCl_3$): λ_{max} (ε / dm^3 mol^{-1} cm^{-1}) 259 (46000), 264 (49000), 277 (47800), 302 (12200), 314 (18600), 328 (32800), 345 (38100) nm. IR (thin film): ν_{max} 3045, 2926, 2855, 1634, 1628, 1593, 1549, 1435, 1406, 1373, 1344, 1296, 1263, 1238, 1198, 1184, 1155, 1123, 1028, 889, 847, 768, 733, 694 cm^{-1}.

Synthesis of platinum (II) complexes

General method for the complexes[17]

A solution of potassium tetrachloroplatinate (II) (1 eq.) in water (2 mL) was added to a stirring solution of HL^n (1 eq.) in 2-ethoxyethanol (6 mL) under dinitrogen and heated to 80 °C for 16 h in a foil-wrapped flask. Brine (10 mL) was added to the cooled solution and the resultant precipitate was collected on a sinter and washed with water (2 × 10 mL) and dried. The solid was used without purification. Crude [Pt(L)-μ-Cl_2Pt(L)] was then dissolved in a minimum volume of DMSO before being precipitated with brine (10 mL), filtered on a sinter and washed with water (2 × 20 mL). [Pt(L)(DMSO)Cl] (1 eq) was dissolved in 3-pentanone (5 mL), to which sodium acetylacetonate (1 – 10 eq) was added. The reaction was stirred at room temperature for 16 h under dinitrogen. The solvent was removed *in vacuo* and the crude product dissolved in dichloromethane (10 mL) and filtered to remove any insoluble salts. The yellow solution was dried *in vacuo*. The crude products were purified by column chromatography (silica) and were eluted as the first yellow band with dichloromethane and dried *in vacuo*.

Synthesis of [Pt(L[1])(acac)]:[17b] using [Pt(L[1])(DMSO)Cl] (0.044 g, 0.066 mmol) and sodium acetylacetonate monohydrate (0.080 g, 0.660 mmol). Obtained as a dark yellow solid. Yield = 0.038 g, (89%). ^{1}H NMR (400 MHz, $CDCl_3$): δ_H 9.43 (1H, d, $^3J_{HH}$ = 8.8 Hz), 8.00 (1H, dd, J_{HH} = 8.4, 1.2 Hz), 7.70 – 7.64 (2H, m), 7.57 (1H, s), 7.51 – 7.47 (1H, m), 7.33 (1H, dd, J_{HH} = 8.0, 1.2 Hz), 7.17 – 7.13 (1H, m), 7.02 – 6.98 (1H, m), 6.66 (1H, br. t, $^3J_{HH}$ = 6.0 Hz, N*H*), 5.57 (1H, s, acac), 3.55 – 3.50 (2H, m), 2.04 (3H, s, acac), 2.03 (3H, s, acac), 1.75 – 1.67 (2H, m), 1.45 – 1.28 (10H, m), 0.91 (3H, t, $^3J_{HH}$ = 6.8 Hz) ppm. ^{13}C{^{1}H} NMR (75.6 MHz, $CDCl_3$): δ_C 185.7, 184.0, 169.3, 166.8, 149.4, 145.7, 144.7, 139.8, 131.0, 129.7, 129.6, 127.1, 126.5, 125.2, 125.1, 124.5, 124.0, 114.2, 101.9, 40.3, 31.9, 29.8, 29.4, 28.5, 27.3, 27.2, 22.8, 14.2 ppm. ^{195}Pt{^{1}H} NMR (107.51 MHz, $CDCl_3$): δ_{Pt} -2776 ppm. MS(ES) found *m/z* = 652.2 [M - H]$^-$. UV-vis ($CHCl_3$): λ_{max} (ε / dm^3 mol^{-1} cm^{-1}) 300 (9920), 349 (2810), 368 (3130), 423 (2420) nm. IR (thin film): ν_{max} 3268 (NH), 1643 (C=O), 1582 (C=O) cm^{-1}.

Synthesis of [Pt(L[2])(acac)]: using [Pt(L[2])(DMSO)Cl] (0.041 g, 0.051 mmol) and sodium acetylacetonate monohydrate (0.062 g, 0.508 mmol). The product was purified by column chromatography (silica) and was eluted as the first yellow band with dichloromethane and dried to yield a dark yellow solid. Yield = 0.034 g, (85%). ^{1}H NMR (400 MHz, $CDCl_3$): *major isomer* δ_H 9.59 (1H, d, $^3J_{HH}$ = 8.4 Hz), 8.39 (1H, d, $^3J_{HH}$ = 8.0 Hz), 7.91 (1H, d, $^3J_{HH}$ = 8.0 Hz), 7.90 (1H, d, $^3J_{HH}$ = 8.4 Hz), 7.90 –7.23 (9H, m), 7.17 – 7.11 (3H, m), 5.71 (1H, d, $^2J_{HH}$ = 14.8 Hz, C*H*H), 5.57 (1H, s, acac), 5.15 (1H, d, $^2J_{HH}$ = 14.8 Hz, CH*H*), 2.80 (2H, app. q), 2.05 (3H, s, acac), 2.03 (3H, s, acac), 1.91 – 0.89 (12H, m), 0.71 (3H, t, $^3J_{HH}$ = 7.2 Hz) ppm; *minor isomer* δ_H 9.56 (1H, d, $^3J_{HH}$ = 8.8 Hz), 7.97 (1H, d, $^3J_{HH}$ = 7.6 Hz), 7.82 – 7.05 (13H, m), 6.95 (1H, app. t), 5.45 (1H, s, acac), 4.89 – 4.78 (2H, br. m, CH_2), 4.22 – 4.05 (1H, br. m), 3.35 – 3.20 (1H, br. m), 2.92 – 2.80 (2H, m), 2.01 (3H, s, acac), 2.00 (3H, s, acac), 1.91 – 0.89 (13H, t, $^3J_{HH}$ = 6.8 Hz) ppm. ^{13}C{^{1}H} NMR (151.2 MHz, $CDCl_3$): *both isomers* δ_C 184.5, 184.4, 183.2, 183.1, 168.8, 168.6, 167.3, 166.7, 148.5, 148.5, 144.8, 144.7, 144.6, 143.8, 139.1, 133.1, 132.8, 130.9, 130.8, 130.3, 130.2, 130.2, 129.7, 129.0, 128.9, 128.6, 128.5, 128.2, 128.0, 128.0, 127.9, 127.9, 127.7, 127.2, 126.5, 126.2, 126.1, 126.0, 125.9, 125.6, 125.4, 123.9, 123.8, 123.7, 123.3, 123.1, 123.0, 123.0, 122.8, 121.0, 114.8, 112.6, 112.1, 100.8, 100.7, 49.1, 46.1, 44.8, 43.9, 34.4, 30.8, 30.6, 28.3, 28.2, 27.9, 27.9, 27.3, 27.3, 27.0, 26.6, 26.2, 26.1, 25.4, 21.6, 21.5, 13.1, 13.0 ppm. ^{195}Pt{^{1}H} (107.51 MHz, $CDCl_3$): δ_{Pt} -2784 ppm. UV-vis ($CHCl_3$): λ_{max} (ε / dm^3 mol^{-1} cm^{-1}) 261 (12500), 273 (12500), 284 (13600), 294 (12700), 342 (4140), 359 (4370), 378 (3070), 406 (2450) nm. IR (thin film): ν_{max} (C=O), 1580 (C=O) cm^{-1}.

Synthesis of [Pt(L[3])(acac)]: using [Pt(L[3])(DMSO)Cl] (0.095 g, 0.111 mmol) and sodium acetylacetonate monohydrate (0.135 g, 1.109 mmol). The product was purified by column chromatography (silica). The product was eluted as the first yellow band with dichloromethane and dried to yield a dark yellow solid. Yield = 0.068 g, (73%). ^{1}H NMR (400 MHz, $CDCl_3$): δ_H 9.58 (1H, d, $^3J_{HH}$ = 8.8 Hz), 8.56 – 8.54 (3H, m), 8.11 (2H, dd, $^3J_{HH}$ = 8.4 Hz, 0.8 Hz), 7.74 – 7.65 (6H, m), 7.59 – 7.55 (2H, m), 7.49 (1H, dd, J_{HH} = 7.6 Hz, 0.8 Hz), 7.38 – 7.34 (1H, m), 7.26 – 7.23 (1H, m), 7.17 – 7.14 (1H, m), 6.27 (1H, d, $^2J_{HH}$ =

15.2 Hz, C*H*H), 5.81 (1H, d, $^{2}J_{HH}$ = 15.2 Hz, CH*H*), 5.56 (1H, s, acac), 2.56 (2H, t, $^{3}J_{HH}$ = 8.0 Hz), 2.04 (3H, s, acac), 2.02 (3H, s, acac), 1.42 – 1.22 (2H, m), 1.13 – 1.04 (2H, m), 0.99 – 0.82 (6H, m), 0.77 (3H, t, $^{3}J_{HH}$ = 7.2 Hz), 0.75 – 0.68 (2H, m) ppm. $^{13}C\{^{1}H\}$ NMR (125.8 MHz, $CDCl_3$): δ_C 185.5, 184.2, 169.8, 167.9, 149.5, 145.8, 145.5, 140.0, 134.1, 133.6, 131.5, 131.4, 131.2, 131.1, 130.9, 130.0, 129.6, 129.5, 129.3, 128.8, 127.2, 127.1, 126.9, 126.8, 126.7, 125.3, 125.0, 124.9, 124.8, 124.2, 124.0, 123.9, 123.0, 113.8, 101.7, 53.4, 46.7, 46.0, 45.4, 39.1, 35.4, 31.4, 30.9, 29.2, 29.0, 28.9, 28.7, 28.6, 28.3, 27.9, 27.2, 26.9, 26.3, 22.6, 22.4, 14.1, 14.0 ppm. $^{195}Pt\{^{1}H\}$ (107.51 MHz, $CDCl_3$): δ_{Pt} -2786 ppm. HR-MS: calcd. for 859.3001 $[C_{44}H_{44}N_2O_4{}^{194}Pt]^+$, found *m/z* = 859.3009. UV-vis ($CHCl_3$): λ_{max} (ε / dm^3 mol^{-1} cm^{-1}) 257 (44000), 298 (14800), 350 (6870), 362 (6930), 368 (7440), 389 (6850), 413 (3860) nm. IR (thin film): ν_{max} 1674 (C=O), 1582 (C=O) cm^{-1}.

Synthesis of [Pt(L^4)(acac)]: using [Pt(L^4)(DMSO)Cl] (0.050 g, 0.057 mmol) and sodium acetylacetonate monohydrate (0.069 g, 0.568 mmol). The product was purified by column chromatography (silica) and was eluted as the first yellow band with dichloromethane and dried to yield a dark yellow solid. Yield = 0.068 g, (73%). ^{1}H NMR (400 MHz, $CDCl_3$): *major isomer* δ_H 9.59 (1H, d, $^{3}J_{HH}$ = 8.4 Hz), 8.63 (1H, d, $^{3}J_{HH}$ = 9.2 Hz), 8.32 – 7.50 (11H, m), 7.41 (1H, d), 7.31 (1H, app. t), 7.16 – 7.08 (3H, m), 6.01 (1H, d, $^{2}J_{HH}$ = 14.4 Hz, C*H*H), 5.56 (1H, s, acac), 5.40 (1H, d, $^{2}J_{HH}$ = 14.8 Hz, CH*H*), 2.86 (2H, app. q), 2.04 (3H, s), 2.02 (3H, s), 1.56 – 1.46 (2H, m), 1.41 – 0.90 (10H, m), 0.78 (3H, t, $^{3}J_{HH}$ = 7.2 Hz) ppm; *minor isomer* δ_H 9.55 (1H, d, $^{3}J_{HH}$ = 8.8 Hz), 8.32 – 7.50 (13H, m), 7.47 (1H, app. t), 7.16 – 7.08 (2H, m), 6.89 (1H, app. t), 5.53 (1H, s, acac), 5.16 – 5.05 (2H, br. m, CH_2), 4.13 – 4.02 (1H, br. m), 3.44 – 3.33 (1H, br. m), 2.01 (3H, s, acac), 2.00 (3H, s, acac), 1.90 – 1.80 (2H, br. m), 1.41 – 0.90 (10H, m), 0.87 (3H, t, $^{3}J_{HH}$ = 7.2 Hz) ppm. $^{13}C\{^{1}H\}$ NMR (125.8 MHz, $CDCl_3$): *both isomers* δ_C 184.5, 184.4, 183.2, 183.1, 168.8, 168.7, 167.2, 166.7, 148.5, 144.8, 144.6, 144.5, 144.0, 139.1, 138.9, 130.6, 130.3, 130.2, 130.1, 129.9, 129.5, 129.0, 128.8, 128.7, 128.6, 128.5, 128.4, 127.5, 127.4, 127.3, 126.9, 126.8, 126.3, 126.2, 126.0, 125.8, 125.3, 125.1, 124.6, 124.5, 124.3, 123.9, 123.8, 123.7, 123.6, 123.5, 123.4, 123.2, 122.9, 122.7, 122.4, 120.2, 112.7, 112.3, 100.8, 100.7, 52.4, 49.2, 46.0, 44.7, 43.9, 30.7, 30.5, 28.7, 28.3, 28.2, 27.9, 27.3, 27.0, 26.5, 26.2, 26.1, 25.4, 21.6, 21.5, 13.1, 13.0 ppm. $^{195}Pt\{^{1}H\}$ (107.51 MHz, $CDCl_3$): δ_{Pt} -2788 ppm. HR-MS: calcd. 883.3001 for $[C_{46}H_{45}N_2O_4{}^{194}Pt]^+$, found *m/z* = 883.3010. UV-vis ($CHCl_3$): λ_{max} (ε / dm^3 mol^{-1} cm^{-1}) 256 (32100), 266 (39400), 278 (48200), 297 (25000), 314 (19900), 329(30300), 345 (38300), 361 (10600), 408 (5330) nm. IR (thin film): ν_{max} 1634 (C=O), 1580 (C=O) cm^{-1}.

Ackowledgements

We thank the staff of the EPSRC Mass Spectrometry National Service (Swansea University) and the National Crystallographic Service at the University of Southampton. Access to the Cardiff University high performance computing facility "ARCCA" is gratefully acknowledged.

Notes and references

[a] *School of Chemistry, Main Building, Cardiff University, Cardiff CF10 3AT. Fax: (+44) 029-20874030; Tel: (+44) 029-20879316; E-mail: popesj@cardiff.ac.uk;* [b] *UK National Crystallographic Service, Chemistry, Faculty of Natural and Environmental Sciences, University of Southampton, Highfield, Southampton, SO17 1BJ, England.*

† Electronic Supplementary Information (ESI) available:

[1] a) A. Barbieri, B. Ventura, R. Ziessel, *Coord. Chem. Rev.*, 2012, **256**, 1732; b) X-Y. Wang, A. Del Guerzo, R.H. Schmehl, *J. Photochem. Photobiol. C: Photochem. Rev.*, 2004, **5**, 55; c) N.D. McClenaghan, Y. Leydet, B. Maubert, M.T. Indelli, S. Campagna, *Coord. Chem. Rev*., 2005, **249**, 1336.

[2] O.S. Wenger, Coord. *Chem. Rev.*, 2015, **282-283**, 150.

[3] G.D. Scholes, *Ann. Rev. Phys. Chem*., 2003, **54**, 57; A. Juris, V. Balzani, F. Barigelletti, P. Belser, A. von Zelewsky, *Coord. Chem. Rev*., 1988, **84**, 85.

[4] a) X. Zhang, T. Yang, S. Liu, Q. Zhao, W. Huang, in Chapter 'Transition-metal complexes for triplet-triplet annihilation-based energy up conversion' in Organometallics and Realted Molecules for Energy conversion. Springer 2015; b) W. Wu, D. Huang, X. Yi, J. Zhao, *Dyes and Pigments*, 2013, **96**, 220.

[5] For example, P. Hammarstrom, B. Kalman, B-H. Jonsson, U. Carlsson, *FEBS Lett*., 1997, **420**, 63; J. Duhamel, *Langmuir*, 2012, **28**, 6527.

[6] A.J. Howarth, M.B. Majewski, M.O. Wolf, *Coord. Chem. Rev.*, 2015, **282-283**, 139.

[7] R.M. Edkins, K. Fucke, M.J.G. Peach, A.G. Crawford, T.B. Marder, A. Beeby, *Inorg. Chem.*, 2013, **52**, 9842.

[8] a) W.Y. Heng, J. Hu, J.H.K. Yip, *Organometallics*, 2007, **26**, 6760; b) J. Hu, J.H.K. Yip, D-L. Ma, K-Y. Wong, W-H. Chung, *Organometallics*, 2009, **28**, 51; c) W.T. Wu, W.H. Wu, S.M. Ji, H.M. Guo, J. Zhao, *Eur. J. Inorg. Chem*., 2010, 4470.

[9] a) O. J. Stacey, S. J. A. Pope, *RSC Adv*., 2013, **3**, 25550; b) A.J. Hallett, N. White, W. Wu, X. Cui, P.N. Horton, S.J. Coles, J. Zhao, S.J.A. Pope, *Chem. Commun*., 2012, **48**, 10838.

[10] A.I. Baba, J.R. Shaw, J.A. Simon, R.P. Thummel, R.H. Schmehl, *Coord. Chem. Rev*., 1998, **171**, 43

[11] For example, W.E. Ford, M.A.J. Rodgers, *J. Phys. Chem*., 1992, **96**, 2917; G.J. Wilso, A. Launikonis, W.H.F. Sasse, A.W.-H. Mau, *J. Phys. Chem. A*, 1997, **101**, 4860; J.A. Simon, S.L. Curry, R.H. Schmehl, T.R. Schatz, P. Piotrowiak, X. Jin, R.P. Thummel, *J. Am. Chem. Soc*., 1997, **119**, 11012; M. Hissler, A. Harriman, A. Khatyr, R. Ziessel, *Chem. Eur. J*., 1999, **5**, 3366; D.S. Tyson, J. Bialecki, F.N. Castellano, *Chem. Commun*., 2000, 2355; J-E.S. Sohna, V. Carrier, F. Fages, E. Amouyal, *Inorg. Chem.*, 2001, **40**, 6061; A.F. Morales, G. Accorsi, N. Armaroli, F. Barigelletti, S.J.A. Pope, M.D. Ward, *Inorg. Chem*., 2002, **41**, 6711; I.M.M de Carvalho, I. de S. Moreira, M.H. Gehlen, *Inorg. Chem*., 2003, **42**, 1525; R. Lincoln, L. Kohler, S. Monro, H.M. Yin, M. Stephenson, R.F. Zong, A. Chouai, R. Dorsey, R. Hennigar, R.P. Thummel, S.A. McFarland, *J. Am. Chem. Soc*., 2013, **135**, 17161; M. Stephenson, C. Reichardt, M. Pinto, M. Wachtler, T. Sainuddin, G. Shi, H. Yin, S. Monro, E. Sampson, B. Dietzek, S.A. McFarland, *J. Phys. Chem. A*, 2014, **118**, 10507.

[12] a) S.A. Denisov, Y. Cudre, P. Verwilst, G. Jonusauskas, M. Marin-Suarez, J.F. Fernandez-Sanchez, E. Baranoff, N.D. McClenghan, *Inorg. Chem*., 2014, **53**, 2677; b) A.J. Howarth, D.L. Davies, F. Lelj, M.O. Wolf, B.O. Patrick, *Inorg. Chem*., 2014, **53**, 11882.

[13] S. Medina-Rodriguez, S.A. Denisov, Y. Cudre, L. Male, M. Marin-Suarez, A. Fernandez-Gutierrez, J.F. Fernandez-Sanchez, A. Tron, G. Jonusauskas, N.D. McClenaghan, E. Baranoff, *Analyst*, 2016, **141**, 3090.

[14] a) I.E. Pomestchenko, C.R. Luman, M. Hissler, R. Ziessel, F.N. Castellano, *Inorg. Chem*., 2003, **42**, 1394; b) E.O. Danilov, I.E. Pomestchnko, S. Kinayyigit, P.L. Gentili, M. Hissler, R. Ziessel, F.N. Castellano, *J. Phys. Chem. A*, 2005, **109**, 2465; c) H. Guo, S. Ji, W. Wu, W. Wu, J. Shao, J. Zhao, *Analyst*, 2010, **135**, 2832.

[15] D.P. Lazzaro, P.E. Fanwick, D.R. McMillan, *Inorg. Chem*., 2012, **51**, 10474.
[16] J.P. Michalec, S.A. Bejune, D.R. McMillin, *Inorg. Chem*., 2000, **39**, 2708.
[17] W. Wu, J. Sun, S. Ji, W. Wu, J. Zhao, H. Guo, *Dalton Trans*., 2011, **40**, 11550.
[18] a) O.J. Stacey, J.A. Platts, S.J. Coles, P.N. Horton, S.J.A. Pope, *Inorg. Chem*., 2015, **54**, 6528; b) J.A. Lowe, O.J. Stacey, P.N. Horton, S.J. Coles, S.J.A. Pope, *J. Organomet. Chem*., 2016, **805**, 87; c) O.J. Stacey, A.J. Amoroso, J.A. Platts, P.N. Horton, S.J. Coles, D. Lloyd, C.F. Williams, A.J. Hayes, J.J. Dunsford, S.J.A. Pope, *Chem. Commun*., 2015, **51**, 12305.
[19] A. Juris, V. Balzani, P. Belser, P. von Zelewsky, *Helv. Chim. Acta* 1981, **64**, 2175.
[20] For a recent article in which the effect of adding dispersion to DFT calculations is discussed, see: L. Castro, E. Kirillov, O. Miserque, A. Welle, L. Haspeslagh, J-F. Carpentier, L. Maron, *ACS Catalysis*, 2015, **5**, 416.
[21] B.D. Ward, S.R. Dubberley, L.H. Gade, P. Mountford, *Inorg. Chem.*, 2003, **42**, 4961.
[22] J.Y. Cho, K.Y. Suponitsky, J. Li, T.V. Tirnofeeva, S. Barlow, S.R. Marder, *J. Organomet. Chem.*, 2005, **690**, 4090.
[23] N. Godbert, T. Pugliese, I. Aiello, A. Bellusci, A. Crispini, M. Ghedini, *Eur. J. Inorg. Chem.*, 2007, 5105.
[24] B.M. Still, P.G.A. Kumar, J.R. Aldrich-Wright, W.S. Price, *Chem. Soc. Rev.*, 2007, **36**, 665.
[25] S. Alvarez, *Dalton Trans*., 2013, **42**, 8617.
[26] M. Frank, M. Nieger, F. Vogtle, P. Belser, A. von Zelewsky, L. de Cola, V. Balzani, F. Barigelletti, L. Flamigni, *Inorg. Chim. Acta*, 1996, **242**, 281.
[27] D.F. Evans, *J. Chem. Soc*., 1957, 1351.
[28] J.S. de Melo, A.J.F.N. Sobral, A.M.D.R. Gonsalves, H.D.Burrows, *J. Photochem. Photobiol. A*, 2005, **172**, 151.
[29] S.J. Coles, P.A. Gale, *Chem. Sci*., 2012, **3**, 683.
[30] *CrystalClear-SM Expert 3.1 b27*, 2013, Rigaku
[31] L. Palatinus, G. Chapuis, *J. Appl. Cryst*., 2007, **40**, 786.
[32] G.M. Sheldrick, *Acta Cryst*., 2015, **C71**, 3.
[33] M.J. Frisch, G.W. Trucks, H.B. Schlegel, G.E. Scuseria, M.A. Robb, J.R. Cheeseman, J.A. Montgomery Jr., T. Vreven, K.N. Kudin, J.C. Burant, J.M. Millam, S.S. Iyengar, J. Tomasi, V. Barone, B. Mennucci, M. Cossi, G. Scalmani, N. Rega, G.A. Petersson, H. Nakatsuji, M. Hada, M. Ehara, K. Toyota, R. Fukuda, J. Hasegawa, M. Ishida, T. Nakajima, Y. Honda, O. Kitao, H. Nakai, M. Klene, X. Li, J.E. Knox, H.P. Hratchian, J.B. Cross, V. Bakken, C. Adamo, J. Jaramillo, R. Gomperts, R.E. Stratmann, O. Yazyev, A.J. Austin, R. Cammi, C. Pomelli, J.W. Ochterski, P.Y. Ayala, K. Morokuma, G.A. Voth, P. Salvador, J.J. Dannenberg, V.G. Zakrzewski, S. Dapprich, A.D. Daniels, M.C. Strain, O. Farkas, D.K. Malick, A.D. Rabuck, K. Raghavachari, J.B. Foresman, J.V. Ortiz, Q. Cui, A.G. Baboul, S. Clifford, J. Cioslowski, B.B. Stefanov, G. Liu, A. Liashenko, P. Piskorz, I. Komaromi, R.L. Martin, D.J. Fox, T. Keith, M.A.Al-Laham, C.Y. Peng, A. Nanayakkara, M. Challacombe, P.M.W. Gill, B. Johnson, W. Chen, M.W. Wong, C. Gonzalez, J.A. Pople, Gaussian 03, Revision E.01. Gaussian, Inc., Wallingford CT, 2004.
[34] a) A.D. Becke, *J. Chem. Phys.*, 1993, **98**, 5648; b) C. Lee, W. Yang, R.G. Parr, *Phys. Rev. B*, 1988, **37**, 785; c) B. Miehlich, A. Savin, H. Stoll, H. Preuss, *Chem. Phys. Lett.*, 1989, **157**, 200.
[35] S. Grimme, J. Antony, S. Ehrlich, H. Krieg, *J. Phys. Chem.*, 2010, **132**, 154104.
[36] W.J. Hehre, R. Ditchfield, J.A. Pople, *J. Chem. Phys.*, 1972, **56**, 2257.
[37] J.D. Routledge, A.J. Hallett, J.A. Platts, P.N. Horton, S.J. Coles, S.J.A. Pope, *Eur. J. Inorg. Chem.*, 2012, 4065.

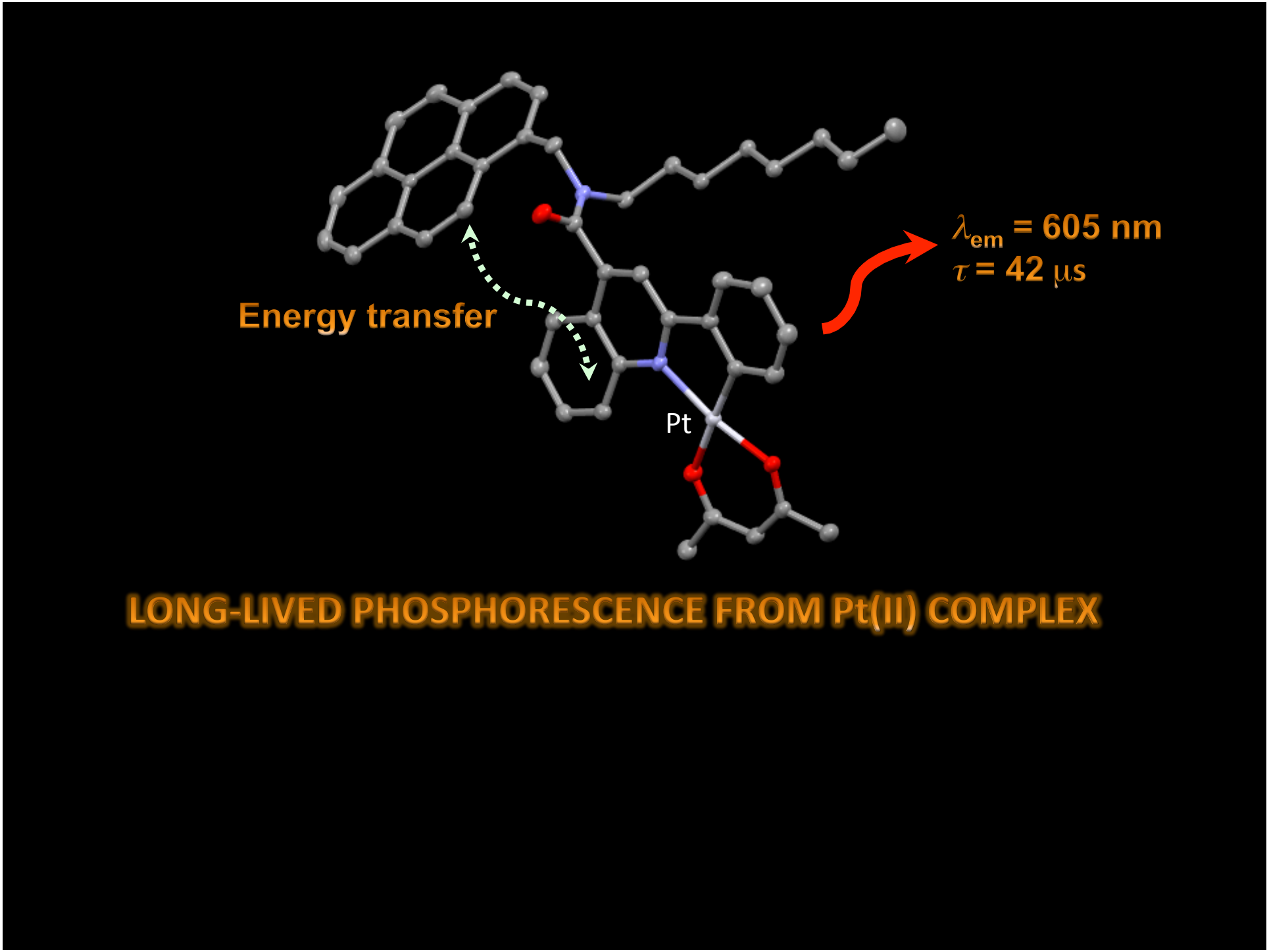
Energy transfer
λ_{em} = 605 nm
τ = 42 μs
Pt
LONG-LIVED PHOSPHORESCENCE FROM Pt(II) COMPLEX